Research Square

Preprints are preliminary reports that have not undergone peer review.
They should not be considered conclusive, used to inform clinical practice,
or referenced by the media as validated information.

Precise microwave ablation in hepatic neoplasms adjacent to high-risk structures: a prospective pilot study

Liping Yang
Puyang Hospital of Traditional Chinese Medicine https://orcid.org/0000-0002-2896-1474
Qinying Li
Puyang Hospital of Traditional Chinese Medicine
Gang Dong
The first affiliated hospital of Zhenzhou University
Lulu Sun
The first hospital of Zhengzhou University
Yan Xia
Puyang Hospital of Traditional Chinese medicine
Longjun Wu
Puyang Hospital of chinese traditional medicine
Gaoang Qi
Puyang hospital of chinense traditioanl medicine
Jianhua Wang
Puyang hospital of chinese tradiotional medicine
Yanjun Song
Puyang hospital of chinese traditional medicine
Jie Yu (jiemi301@163.com)
Chinese People's Liberation Army General Hospital
Ping Liang
Chinese people Liberation Army Genenral Hospital

Research

Keywords: Microwave ablation, Hepatic neoplasms, Artificial pleural effusion and ascites, Three-dimensional thermal field, High-risk structures

Posted Date: October 20th, 2020

DOI: https://doi.org/10.21203/rs.3.rs-69363/v1

License: This work is licensed under a Creative Commons Attribution 4.0 International License. Read Full License

Abstract

Objective

To evaluate the safety and efficiency of ultrasound (US)-guided precise MWA assisted by artificial pleural effusion and/or ascites in hepatic neoplasms adjacent to high-risk structures based on a 3D preoperative planning system.

Methods

Twenty-five patients with hepatic neoplasms adjacent to high-risk structures were enrolled. CT images of all patients were reconstructed with 3D visualization software for preoperative planning. The puncture path and needle layout were estimated. US-guided precise MWA assisted by artificial pleural effusion and/or ascites was performed. Patients were followed by clinical and imaging examinations at 3, 6, and 12 months after the MWA. Study outcomes including complications, liver function, AFP level, and ablation lesion volumes were evaluated.

Results

Thirty-two tumors in 25 patients underwent precise MWA. Except for 4 patients with tumors near the macrovascular, 21 patients received artificial pleural effusion and/or ascites, achieving a complete separation. Based on preoperative 3D planning, patients with tumors near the diaphragmatic dome underwent administration of artificial pleural effusion and ascites, while patients with tumors near the gastrointestinal tract or gallbladder received artificial ascites. Of the 32 tumors, 30 achieved complete ablation in the first MWA session, and 29 achieved conformal ablation with a safe boundary of 0.5-1 cm. No severe complications were observed. Only one tumor exhibited local progression. Moreover, serum levels of ALT, AST and AFP were significantly decreased during the follow-up period.

Conclusion

Based on the 3D preoperative planning system, US-guided precise MWA assisted by artificial pleural effusion and ascites, is a safe and effective tool to treat hepatic neoplasms adjacent to high-risk structures.

Introduction

Liver cancer is the fourth leading cause of cancer-related death worldwide. There were approximately 841,000 newly diagnosed cases and 782,000 deaths reported in 2018[1]. Despite advancements in diagnostic and treatment strategies for liver cancer, the prognosis remains poor due to the low percentage (10–20%) of radically resectable liver cancer. Thus, the identification of novel and safe strategies would represent a major advance for the treatment of liver cancer.

Locoregional ablation therapy has been recommended as a first-line treatment option for early stage or unresectable liver cancer according to updated therapy guidelines. Among the various ablation therapy methods, microwave ablation (MWA), as a minimally invasive strategy, has become an effective methods in the comprehensive treatment of liver cancer [2]. Microwave ablation kills cancer cells using high frequency electromagnetic waves to oscillate polar molecules and ions, thereby causing degeneration and necrosis of the affected protein and alterations in the cell structure[3]. Due to obvious advantages including convenience, real-time imaging and radiation-free imaging, ultrasound (US) has been one of the most widely used guiding methods. However, due to the poor acoustic window and vulnerability to thermal damage, there are still many challenges for US-guided microwave ablation in patients with tumors adjacent to high-risk structures such as the macrovasculature, diaphragmatic dome, gastrointestinal tract and gallbladder, which significantly limit the application of microwave ablation for liver cancer.

Artificial pleural effusion and ascites have been widely used as ancillary methods to create a liquid barrier and to separate the tumor from vital organs [4, 5]. It enables a clear display of lesions on the two-dimensional color ultrasound and provides a sufficient safe space for microwave ablation treatment. Three-dimensional (3D) reconstruction techniques offer the visualization of complex longitudinal architecture in composite displays. The progress in computer hardware and software technology has significantly

shortened the reconstruction process and reduced operator interaction, generating 3D images with delineation of mural anatomy and pathology [6]. Precise preprocedural planning and continuous quality control could provide substantial information on the accuracy of surgical reconstruction and device implantation [7]. Scientific preoperative planning based on 3D reconstruction techniques combined with artificial pleural effusion and/or ascites significantly improves the efficacy and feasibility of precise microwave ablation for liver cancer.

In this prospective study, 25 patients with hepatic neoplasms adjacent to high-risk structures were enrolled. Preoperative treatment planning was performed by a 3D thermal field. The feasibility, efficacy and safety of imaging-guided precise microwave ablation assisted by artificial pleural effusion and ascites were evaluated.

Materials And Methods

Patient enrollment

Twenty-five patients with hepatic neoplasms adjacent to high-risk structures who were treated with US-guided microwave ablation were enrolled from June 2016 to June 2018. The inclusion criteria were as follows: For liver nodules with a diameter of ≤ 2 cm, liver tissue biopsy confirmed the diagnosis of primary liver cancer or metastatic liver cancer; for liver nodules with a diameter > 2 cm, the typical imaging manifestations on contrast-enhanced CT or MRI combined with serum AFP > 200 ng/ml confirmed liver cancer. The distance between the tumors and high-risk structures was ≤ 5 mm or the tumor could not be completely visualized. The patients had not undergone ablation therapy, or the patients presented new tumors after treatment. The following patients were excluded: patients who had a tumor diameter > 5 cm; patients who presented poor coagulation function and a poor liver function reserve; patients who had a massive effusion in the abdominal cavity; patients who presented distant metastasis of liver cancer; patients who could not tolerate surgery; and patients who refused to participate in this study. This prospective pilot study was approved by the Institutional Review Board of the Puyang Hospital of Traditional Chinese Medicine. All participants signed written informed consent upon enrolment.

Three-dimensional thermal field-based preoperative planning

Two-dimensional image information was obtained from all patients by upper-abdominal plain scanning and three-phase enhanced scanning using 64-slice spiral CT. The images were reconstructed and analyzed by 3D visualization software (Kangyou Company). The 3D reconstruction models were observed from multiple angles, which clearly showed the anatomical relationship of the intrahepatic duct system, as well as the adjacent relationship between the tumor and high-risk structures. According to the 3D model, the shortest puncture pathway was designed, and the optimal puncture pathway was planned to avoid blood vessels and to ensure going through 1 cm of normal liver tissue when entering the needle. The layout of the ablation needle was planned as follows: single-needle ablation or multi-needle ablation; how to minimize the number of needle movements when performing single needle ablation; how to select parallel needles, crosswise needles, or angled needles when performing multi-needle ablation; how to achieve conformal tumor ablation according to the range of the ablation heat field and the size of the tumors; and how to adjust the ablation zone to completely cover the tumor. The safe boundary of the ablation thermal field was kept at 0.5-1 cm to avoid damage to the adjacent organs.

Application of artificially induced pleural effusion and/or ascites

The patients adopted the supine position or left lateral decubitus position. The positional relationship between the tumor and adjacent vital organs was observed under ultrasound. A detailed plan of artificial injection of normal saline to induce pleural effusion and/or ascites was designed. The needle insertion point was selected to avoid important organs according to the preoperative plan. Infiltration anesthesia was performed using 2% lidocaine.

For patients with tumors adjacent to the diaphragmatic dome, artificial pleural effusion was induced by injecting saline into the right pleural cavity under ultrasound guidance. Similarly, artificial ascites was induced by injecting saline into the right abdominal cavity through a peripherally inserted central catheter (PICC) under ultrasound guidance. The fluid sonolucent area in the abdominal cavity was closely observed under ultrasound. After a certain depth was reached, an indwelling drainage tube was left in the abdominal cavity. The saline inlet tube and the drainage tube were connected together to keep injecting saline so that the tumor was completely displayed and sufficient treatment space between the tumor and adjacent vital organs was guaranteed.

Additionally, for patients with tumors adjacent to the gallbladder, the 21 GPTC needle was used to inject saline between the tumor and the gallbladder wall to separate both under ultrasound guidance. Similarly, for patients with tumors closely adherent to the gallbladder, saline was injected between the serosal and muscular layers to ensure a safe ablation distance of at least 10 mm.

Ultrasound-guided microwave ablation

A microwave ablation treatment machine (KY-2000, Nanjing Kangyou Medical Technology Co., Ltd.) was used, and an electrode needle with an outer diameter of 14 G was selected. The transmission frequency was set at 2450 MHz. The electrode needle was connected with the water-cooled antenna, and the output power was set from 1 W to 100 W (continuously adjustable).

The patients were placed in the supine position or left lateral decubitus position, and intravenous anesthesia was performed. According to the preoperative 3D plan, the optimal puncture point was selected under the guidance of color Doppler ultrasound (Philips ETIQ7). The conventional disinfection and surgical drape were conducted. The skin at the selected puncture point was cut open by 2 mm. The 14G microwave electrode needle was inserted according to the plan. The output power was adjusted so that the coagulation necrosis temperature of the tumor tissue reached 60 °C immediately or 50 °C for 3 minutes. During the treatment, an ablation temperature measurement probe was used to detect the ablation temperature in real time, and the entire tumor was covered by the ablation zone. After the treatment, the needle pathway was fully burned to avoid bleeding and tumor metastasis.

Observation indicators

The feasibility, efficacy and safety of imaging-guided precise microwave ablation were evaluated. Twenty-four hours after the operation, all patients underwent contrast-enhanced MRI, and no detection of any enhancement signal in the ablation-targeted zone was thought to indicate complete ablation of the tumor; an area of enhancement inside or near the ablation-targeted zone was believed to be indicate incomplete ablation. Meanwhile, the adverse events of precise microwave ablation, including reactive pleural effusion, fever, abdominal pain, hemopneumothorax, intestinal perforation, and bile leakage, were recorded. The patients were followed up at 3 months, 6 months and 12 months. Liver function parameters, serum AFP level, ablation lesion diameter and volumes were estimated.

Statistical analysis

The measurement data are expressed as the mean ± standard deviation (SD). Continuous variables were analyzed with the Wilcoxon rank sum test between the two groups. One-way ANOVA was used to compare the differences among the three groups. Categorical variables were compared by Fisher's exact test. A P value less than 0.05 was designated as statistically significant. Statistical analyses were performed using SPSS version 20.0 for Windows (SPSS, Inc., Chicago, IL).

Results

Patient characteristics

Twenty-five patients with 32 hepatic neoplasms adjacent to high-risk structures were eligible for this study. As presented in Table 1, the mean (SD) age of the cohort was 54.2 (9.81) years, and the subjects consisted of 7 women and 18 men. The mean (SD) body mass index was 20.2 (2.19). In addition, the average levels of serum ALT and AST were 109.0 U/L (SD 107.12) and 109.0 U/L (SD 102.0), respectively. The average value of serum AFP was 570.4 ng/ml (SD 403.7). Regarding the tumor locations, there were 11 tumors near the diaphragmatic dome in 8 patients, 10 tumors near the gastrointestinal tract in 9 patients, 5 tumors near the gallbladder in 4 patients, and 6 tumors near large blood vessels in 4 patients. The average maximum tumor diameter in each patient was 31.5 mm (SD 9.13), and the average ablation time in all patients was 5.37 minutes (SD 1.79).

Table 1. The clinical features of patients and characteristics of liver tumor

Cases	Gender	Age (yrs)	BMI	ALT (U/L)	AST (U/L)	AFP (ng/ml)	Clinical staging in Barcelona	Child-Pugh score	Max tumor dia (mm)	Tumor volume (ml)	Tumor location	Diagnosis	Ablation time (s)	Applicator insertion
case_1	male	64	18.1	28	20	609.3	B	B	43	33540	nearby diaphragm	HCC	410	2
case_2	male	42	19.5	43	33	531.5	A4	A	24	4537	nearby diaphragm	HCC	250	1
case_3	male	38	19.4	88	64	345.6	A1	A	23	4811	nearby diaphragm	HCC	270	1
case_4	female	49	22.6	28	56	3.28	A2	A	32	11652	nearby diaphragm	HCC	230	2
case_5	male	45	24.3	73	92	912.3	A1	A	45	34965	nearby diaphragm	HCC	430	2
case_6	female	55	24.5	83	76	784.5	A3	B	37	21372	nearby diaphragm	HCC	410	2
case_7	male	63	17.8	277	357	1148.1	B	B	48	46366	nearby diaphragm	HCC	570	2
case_8	male	44	20.4	94	25	254.6	A1	A	34	14671	nearby diaphragm	HCC	270	2
case_9	female	32	18.7	27	23	694.1	0	A	20	2699	nearby gastrointestinal tract	HCC	290	1
case_10	female	64	18.1	20	23	415.6	A3	A	22	4157	nearby gastrointestinal tract	HCC	240	1
case_11	male	62	19.2	32	17	12.08	A4	A	25	5752	nearby gastrointestinal tract	HCC	275	1
case_12	male	68	18.3	96	104	484	B	B	34	16266	nearby gastrointestinal tract	HCC	250	2
case_13	male	54	17.3	107	108	573.3	A3	B	32	12531	nearby gastrointestinal tract	HCC	240	2
case_14	male	53	21.2	99	87	891.4	A1	A	26	8736	nearby gastrointestinal tract	HCC	315	1
case_15	female	53	19.9	79	54	20.58	A1	A	42	29404	nearby gastrointestinal tract	HCC	460	2
case_16	male	60	22.2	43	61	209.1	A2	A	38	20619	nearby gastrointestinal tract	HCC	310	2
case_17	male	67	21.7	335	297	1087.6	A3	B	50	51603	nearby gastrointestinal tract	HCC	600	2
case_18	male	46	22.8	24	220	294.6	A4	A	27	7724	nearby gallbladder	HCC	290	1
case_19	female	51	23.2	21	38	369.4	0	A	18	1731	nearby gallbladder	HCC	180	1
case_20	male	58	21.1	65	58	530.2	A2	A	25	6038	nearby gallbladder	HCC	280	1
case_21	male	63	18	153	198	809.2	A3	B	26	6551	nearby gallbladder	HCC	295	1
case_22	male	59	18.8	184	201	13.9	A4	A	30	9724	nearby large blood vessels	HCC	245	2
case_23	male	42	21.5	236	94	1041	0	A	19	2908	nearby large blood vessels	HCC	200	1
case_24	female	57	19.4	54	67	619.4	A2	A	31	10880	nearby large blood vessels	HCC	340	2
case_25	male	65	17.1	435	352	1605	C	B	36	20203	nearby large blood vessels	HCC	400	2

Tumor characteristics

Regarding the locations, there were 11 neoplasms near the diaphragmatic dome in 8 patients, 10 tumors near the gastrointestinal tract in 9 patients and 4 tumors near the gallbladder in 4 patients. The representative enhanced CT images showed the tumors from different visual angles, including the cross section, vertical plane and coronal plane, which clearly presented the tumor diameter and location, as well as the distance between the tumor and adjacent structures (Fig. 1A, Fig. 2A-2C, Fig. 3A-3C). The ablation range totally covered the tumor boundary in the 3D visualization software (Fig. 1B, Fig. 2D-F and Fig. 3D). Furthermore, original CT images were exported, and simulations of the pathways of the ablation needle were performed on enhanced CT images from different levels (Fig. 1C, Fig. 2G and Fig. 3E). To further improve the accuracy of punctured pathways and reduce injury to the adjacent viscera, simulations of punctured pathways and the ablation range were performed in the liver alone, the neighboring relationship among the ablation range and intrahepatic bile duct and gallbladder were separately analyzed, and the optimal punctured pathway was selected (Fig. 1D, Fig. 2H and Fig. 3F).

Safety outcome

Among the 25 patients, six had minor complications after ablation. One patient underwent postoperative reactive pleural effusion with 500 ml fluid, which was discharged by thoracic cavity drainage. Three patients experienced fever less than 38.5℃, and all of them recovered after treatment with physical cooling. Two patients suffered from abdominal pain, which disappeared after symptomatic treatment. In addition, no patients with serious complications, such as hemopneumothorax, intestinal perforation, and bile leakage, were observed.

Efficacy outcomes

Based on 3D thermal field preoperative treatment planning, 25 patients were treated with US-guided MWA, which was assisted by artificial pleural effusion and/or ascites. The results from the contrast-enhanced MRI scan at 24 hours after the operation showed that 30 tumors were completely eradicated once, and the radical resection rate reached 93.7% (30/32). Of those tumors, 29 tumors achieved a conformal ablation in which the safety ablation boundary remained between 0.5 cm and 1.0 cm, and the safety ablation rate was 90.6% (29/32). However, due to its complicated structure and location, one tumor near the gastrointestinal tract required an additional MWA session to maximize the efficacy of the treatment. The tumor did not present local progression during the follow-up period. The other tumor near the macrovasculature did not achieve complete ablation because of portal vein invasion. Local progression of the tumor was observed after 3 months of follow-up.

The dynamic alteration of liver function, serum AFP level, ablation lesion diameter and volumes during the follow-up period is shown in **Supplementary data file 1**. There was a significant decrease in serum levels of ALT and AST within the first 6 months after MWA, and then it gradually dropped to normal at 12 months (Fig. 4A and 4B). Notably, except for one patient who presented with tumor progression, the serum level of AFP was remarkably decreased to the normal level during the first 3 months, which suggested complete ablation of the tumors (Fig. 4C). Furthermore, we further evaluated the diameter and volume of the ablated lesions. Compared with the preoperative values, the maximum diameter and volume of the ablated lesions significantly decreased at 12 months (Fig. 4D and 4E). Moreover, the reduced ratio of tumor volume was consistently increased at 6 and 12 months compared with the ratio at the first 3 months (Fig. 4F), which suggested that the assimilation of necrotic tissues became accelerated from 3 months postoperatively.

Discussion

This study demonstrates a safe and effective profile of US-guided MWA combined with artificial pleural effusion and/or ascites in the treatment of hepatic neoplasms adjacent to high-risk structures. There were no major complications, and only six cases with minor complications among 25 patients were treated with MWA. The serum levels of ALT, AST and AFP remarkably decreased after ablation for 3, 6, and 12 months, respectively. Furthermore, the volume reduction ratio of the ablation lesions considerably increased during the follow-up period.

As a minimally invasive and effective treatment, microwave ablation has been characterized as a simple operation that causes less trauma and is repeatable; moreover, it has been identified as one of the major curative methods for liver cancer [8]. Recently, it has been widely accepted that the therapeutic effect of minimally invasive treatment is equal to that of radical resection [9] and that minimally invasive treatment is less invasive and promotes quick recovery [10, 11]. Our previous studies have elucidated that the cumulative 1-, 3-, and 5-year survival rates are 92%, 72%, and 51% in 288 patients with liver cancer treated with microwave ablation, respectively [12]. However, due to the limitation of ultrasound, hepatic neoplasms adjacent to high-risk structures such as the gastrointestinal tract, gallbladder, diaphragm and macrovessels may not be clearly displayed, which has become a great challenge in ultrasound-guided microwave ablation. Artificial pleural effusion and ascites have been reported to improve the visibility of ultrasound and reduce the relevant complications during ablation treatment [13]. The injected ascites is absorbed within one week in most patients [14]. Additionally, to overcome the shortcomings of 2D imaging techniques, 3D-based thermal ablation has been applied in preoperative treatment planning. Previous studies have addressed the problem of modeling the thermal field of microwave ablation theoretically, and a simple approach for preoperative planning of MWA has been developed [15, 16]. Doctors can repeatedly perform surgical planning on individualized 3D models, optimize surgical plans, and improve surgical skills and safety. This novel modality not only complies with surgeons' operating habits, but also avoids the defect of inaccurate judgment in the ultrasound-guided 2D space [17]. Based on the 3D thermal field preoperative planning, the ablation needle layout, ablation thermal field range and ablation duration are planned ahead, which could minimize the ablation needle insertion pathways and avoid the risk of repeated puncture [18,

19]. Consistently, in our study, we combined 3D image processing and analysis methods, trajectory planning, and thermal modeling planning with navigation technology to establish a 3D visualization preoperative treatment planning system for microwave ablation of hepatic neoplasms adjacent to high-risk structures. Moreover, the success rate of artificial pleural effusion and ascites injection was 88–100%, and no serious complications related to artificial ascites injection occurred. Furthermore, 21 patients achieved a successful separation of liver tumors from adjacent high-risk structures, which provided sufficient space for microwave ablation and ensured subsequent operation. Moreover, the artificial pleural effusion and ascites were completely absorbed within 3 days after microwave ablation. Assisted by artificial pleural and ascites, MWA achieved a radical resection rate of 93.7% with a good prognosis during the follow-up period. Therefore, the application of a 3D visualization preoperative treatment planning system for MWA in hepatic neoplasms assisted by artificial pleural effusion and ascites could serve as a safe and effective method.

Minimally invasive microwave or radiofrequency ablation procedures have a significantly lower rate of complications than surgery has. Several major complications, including liver abscess, empyema, bile duct injury, colon perforation, tumor seeding, hemorrhage and skin burns, mainly occur in neoplasms adjacent to high-risk structures [20]. For instance, liver cancer adjacent to high risk sites, has a high probability of diaphragm perforation or abdominal cavity organ perforation after microwave ablation, which could also lead to acute peritonitis, severe abdominal infection, multiorgan failure, and other severe complications [21]. Meanwhile, liver tumors abutting high-risk locations such as large blood vessels, extrahepatic heat-sensitive organs and the hepatic caudate lobe are prone to cause thermal ablation damage. Furthermore, ultrasound cannot penetrate gas or bone, which has a great influence on microwave ablation and limits the treatments for tumors at special locations [22, 23]. In this study, artificial pleural effusion and/or ascites injections were successfully performed, and only a few treated patients had minor complication and all recovered with symptomatic treatment, suggesting that US-guided microwave ablation assisted by artificial pleural effusion and ascites is a safe and effective adjuvant treatment strategy that can reduce damage to high-risk near tumors.

Conclusion

In conclusion, this study proposes precision microwave ablation based on 3D thermal field preoperative treatment planning system and artificial pleural effusion and ascites, which would be a safe and effective option for liver tumors adjacent to high-risk areas.

Declarations

Competing interests:

No potential conflict of interest was reported by the author(s).

Consent for publication:

Not applicable.

Availability of data and materials:

Please contact the corresponding author for all data requests.

Funding: The study was supported by the National 13th Five-year Key Research and Development Program of China (2017YFC0112000).

Authors' Contributors: YJ, LP and YL designed the study. YL, LQ, DG, SL, XY, and WL performed the operations, managed the patients and collected clinical data; YL, LQ, QG, WJ and SY analyzed the data. YL and LQ wrote the manuscript. All authors reviewed and approved the manuscript.

Ethical Approval and Consent to participate : The study was approved by the Institutional Review Board of the Puyang Hospital of Traditional Chinese Medicine. All participants signed written informed consents upon enrolment.

Authors' information: [1] Department of Ultrasound Intervention, Puyang Hospital of Traditional Chinese Medicine, Puyang 457000, Henan Province, China; [2] Department of Ultrasound, the First Affiliated Hospital of Zhengzhou University, Zhengzhou 450052, China; [3] Department of Interventional Ultrasound, Chinese People's Liberation Army General Hospital, Beijing 100853, China;

Acknowledgements: Not applicable.

References

1. Bray F, Ferlay J, Soerjomataram I, et al. Global cancer statistics 2018: GLOBOCAN estimates of incidence and mortality worldwide for 36 cancers in 185 countries. Cancer J Clin. 2018;68(6):394–424.
2. Kobayashi T, Aikata H, Kobayashi T, et al: Patients with early recurrence of hepatocellular carcinoma have poor prognosis. *Hepatobiliary & Pancreatic Diseases International*, 16(3):288.
3. EASL Clinical Practice Guidelines. Management of hepatocellular carcinoma. Journal of hepatology. 2018;69(1):182–236.
4. Heimbach JK, Kulik LM, Finn RS, et al. AASLD guidelines for the treatment of hepatocellular carcinoma. Hepatology. 2018;67(1):358–80.
5. Xie C, Duffy AG, Mabry-Hrones D, et al. Tremelimumab in Combination With Microwave Ablation in Patients With Refractory Biliary Tract Cancer. Hepatology. 2019;69(5):2048–60.
6. Nault JC, Sutter O, Nahon P, et al. Percutaneous treatment of hepatocellular carcinoma: State of the art and innovations. Journal of hepatology. 2018;68(4):783–97.
7. Chu KF, Dupuy DE. Thermal ablation of tumours: biological mechanisms and advances in therapy. Nature reviews Cancer. 2014;14(3):199–208.
8. Kondo Y, Yoshida H, Tateishi R, et al. Percutaneous radiofrequency ablation of liver cancer in the hepatic dome using the intrapleural fluid infusion technique. Br J Surg. 2008;95(8):996–1004.
9. Zhang D, Liang P, Yu X, et al. The value of artificial pleural effusion for percutaneous microwave ablation of liver tumour in the hepatic dome: a retrospective case-control study. International journal of hyperthermia: the official journal of European Society for Hyperthermic Oncology North American Hyperthermia Group. 2013;29(7):663–70.
10. Roelandt JR, di Mario C, Pandian NG, et al. Three-dimensional reconstruction of intracoronary ultrasound images. Rationale, approaches, problems, and directions. Circulation. 1994;90(2):1044–55.
11. Bartel T, Rivard A, Jimenez A, et al. Medical three-dimensional printing opens up new opportunities in cardiology and cardiac surgery. European heart journal. 2018;39(15):1246–54.
12. Karanicolas PJ, Jarnagin WR, Gonen M, et al. Long-term outcomes following tumor ablation for treatment of bilateral colorectal liver metastases. JAMA surgery. 2013;148(7):597–601.
13. Liu SR, Liang P, Yu XL, et al. Percutaneous microwave ablation for liver tumours adjacent to the marginal angle. International journal of hyperthermia: the official journal of European Society for Hyperthermic Oncology North American Hyperthermia Group. 2014;30(5):306–11.
14. Liang P, Yu J, Yu XL, et al. Percutaneous cooled-tip microwave ablation under ultrasound guidance for primary liver cancer: a multicentre analysis of 1363 treatment-naive lesions in 1007 patients in China. Gut. 2012;61(7):1100–1.
15. An C, Li X, Liang P, et al. A tumor map generated from three-dimensional visualization of image fusion for the assessment of microwave ablation of hepatocellular carcinoma: a preliminary study. Cancer management research. 2019;11:1569–78.
16. Xu EJ, Lv SM, Li K, et al. Immediate evaluation and guidance of liver cancer thermal ablation by three-dimensional ultrasound/contrast-enhanced ultrasound fusion imaging. International journal of hyperthermia: the official journal of European Society for Hyperthermic Oncology North American Hyperthermia Group. 2018;34(6):870–6.
17. Lachenmayer A, Tinguely P, Maurer MH, et al. Stereotactic image-guided microwave ablation of hepatocellular carcinoma using a computer-assisted navigation system. Liver international: official journal of the International Association for the Study of the Liver. 2019;39(10):1975–85.
18. Liu W, Zheng Y, He W, et al. Microwave vs radiofrequency ablation for hepatocellular carcinoma within the Milan criteria: a propensity score analysis. Aliment Pharmacol Ther. 2018;48(6):671–81.
19. Liu F, Liang P, Yu X, et al. A three-dimensional visualisation preoperative treatment planning system in microwave ablation for liver cancer: a preliminary clinical application. International journal of hyperthermia: the official journal of European Society for Hyperthermic Oncology North American Hyperthermia Group. 2013;29(7):671–7.
20. An C, Cheng Z, Yu X, et al. Ultrasound-guided percutaneous microwave ablation of hepatocellular carcinoma in challenging locations: oncologic outcomes and advanced assistive technology. International journal of hyperthermia: the official journal of

European Society for Hyperthermic Oncology North American Hyperthermia Group. 2020;37(1):89–100.
21. Yu J, Yu XL, Han ZY, et al. Percutaneous cooled-probe microwave versus radiofrequency ablation in early-stage hepatocellular carcinoma: a phase III randomised controlled trial. Gut. 2017;66(6):1172–3.
22. Shibata T, Iimuro Y, Yamamoto Y, et al. Small hepatocellular carcinoma: comparison of radio-frequency ablation and percutaneous microwave coagulation therapy. Radiology. 2002;223(2):331–7.
23. Liang P, Dong B, Yu X, et al. Prognostic factors for survival in patients with hepatocellular carcinoma after percutaneous microwave ablation. Radiology. 2005;235(1):299–307.

Figures

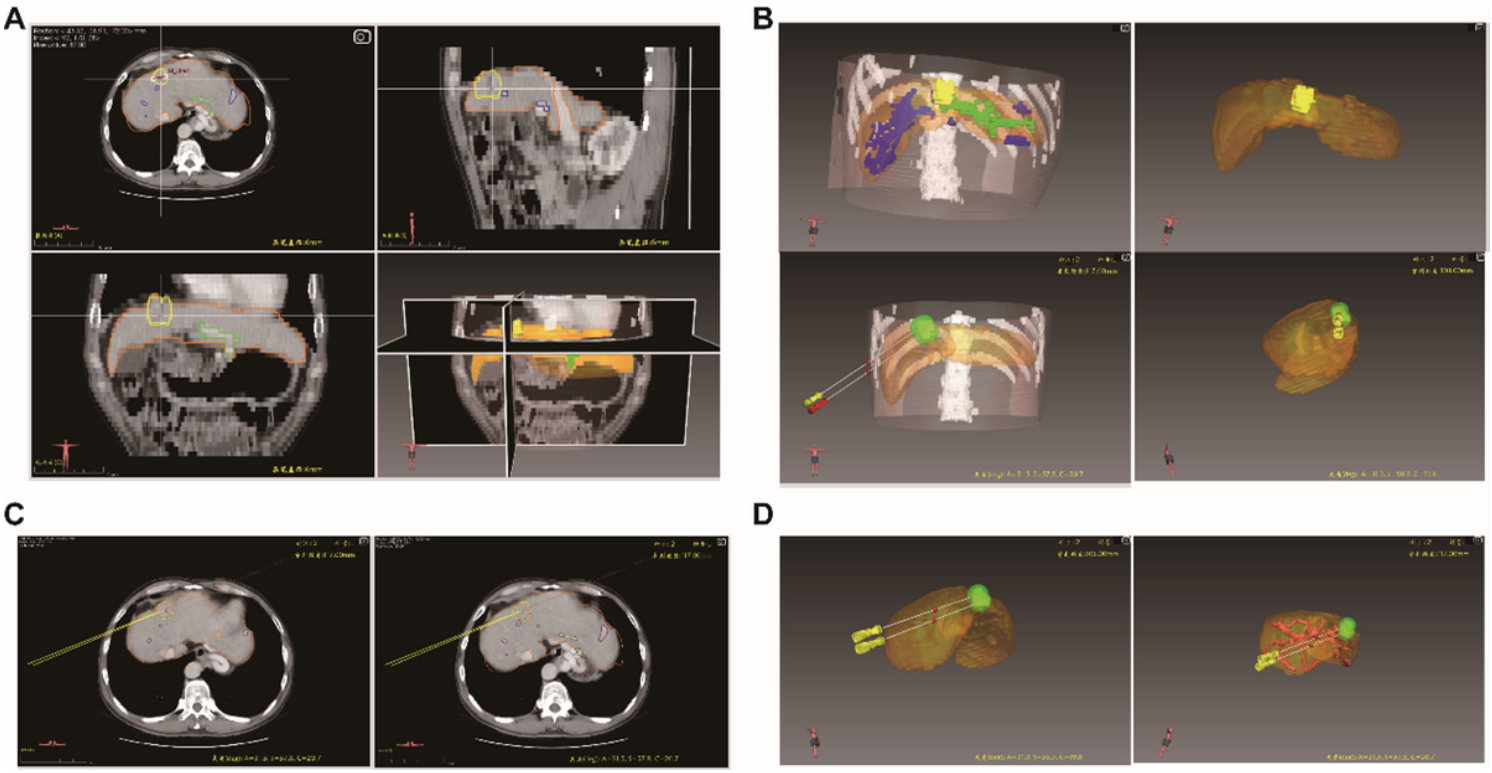


Figure 1

Precise microwave ablation liver tumor nearby the diaphragmatic dome. (A) The enhanced CT images of the tumor from the different visual angles, including cross section, vertical plane and coronal plane were imported, and the 3D visual structure of the tumor was synthesized. (B) The morphology and location of the tumor were re-constructed in the 3D visualization software, and the punctured pathway and the ablation range were simulated. (C) The original CT images were exported, and the simulated pathways were performed on the enhanced CT images from the different levels. (D) The simulations of the punctured pathways and ablation range were performed in the liver alone, and the neighboring relationship between the ablation range and intrahepatic bile duct were separately analyzed.

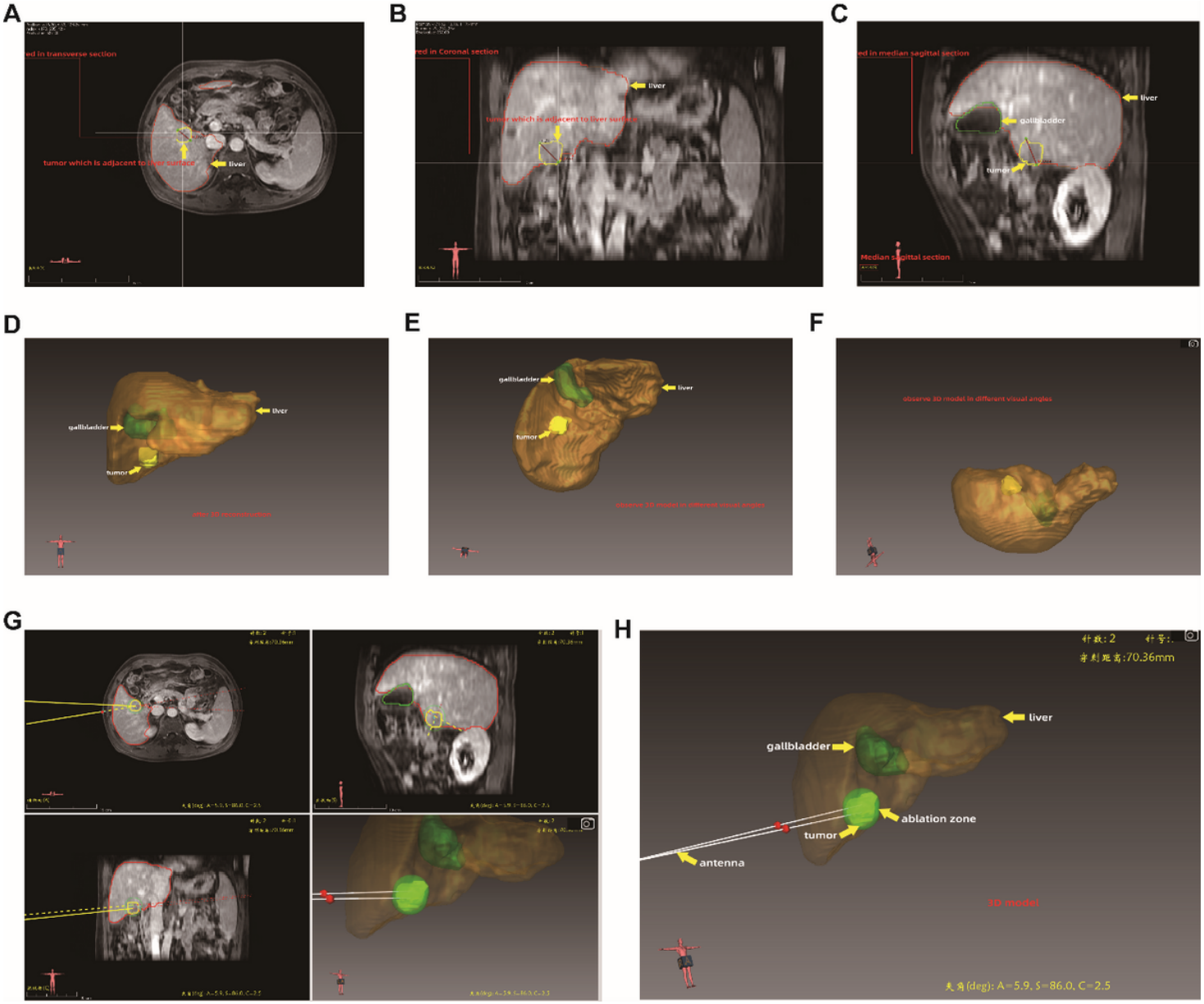


Figure 2

Precise microwave ablation of liver tumors near the gastrointestinal tract. Representative CT images of the tumor are shown from different visual angles, including the cross section (A), coronal plane (B) and vertical plane (C). The major axis and minor axis of the tumor were measured, and the boundaries of the tumor and the liver were drawn and analyzed. After 3D thermal field reconstruction, the tumor location in the liver was clearly observed, and the distance between the tumor and the gallbladder was clearly visual from the different visual angles (D, E and F). (G) The punctured pathway of the ablation needle and the ablation range were simulated in the enhanced CT images from the different visual angles, including the cross section, vertical plane and coronal plane. (H) The needle spacing, puncture pathway, ablation zone, as well as the neighboring relationship between the ablation zone and the gallbladder, were analyzed.

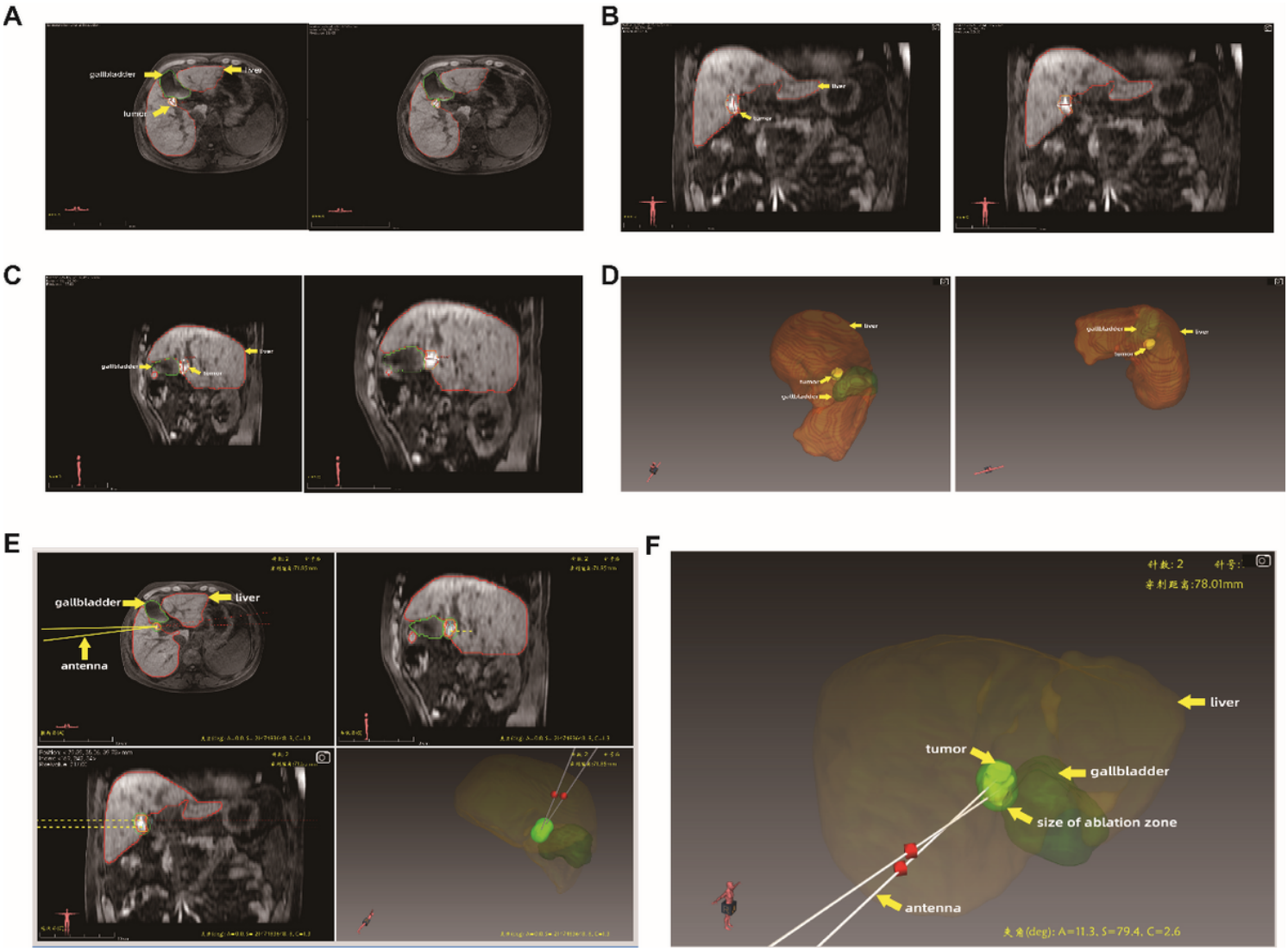


Figure 3

Precise microwave ablation of the liver tumor near the gallbladder. The anatomical structures of and neighboring relationships among the liver, the tumor and the gallbladder are shown. The morphology and position of the tumor were clearly indicated from the different visual angles, including the cross section (A), coronal plane (B) and vertical plane (C) on the CT images. (D) The images of the 3D thermal field were reconstructed, the boundaries of the tumor and liver were clearly observed, and the distance between the tumor and the gallbladder was clearly visual. (E) The punctured pathway of the ablation needle was simulated, and the range of ablation was calculated in the enhanced CT images from the different visual angles, including the cross section, vertical plane and coronal plane. (F) The needle spacing, puncture pathway, ablation zone, and the neighboring relationship between the ablation zone and the gallbladder were analyzed.

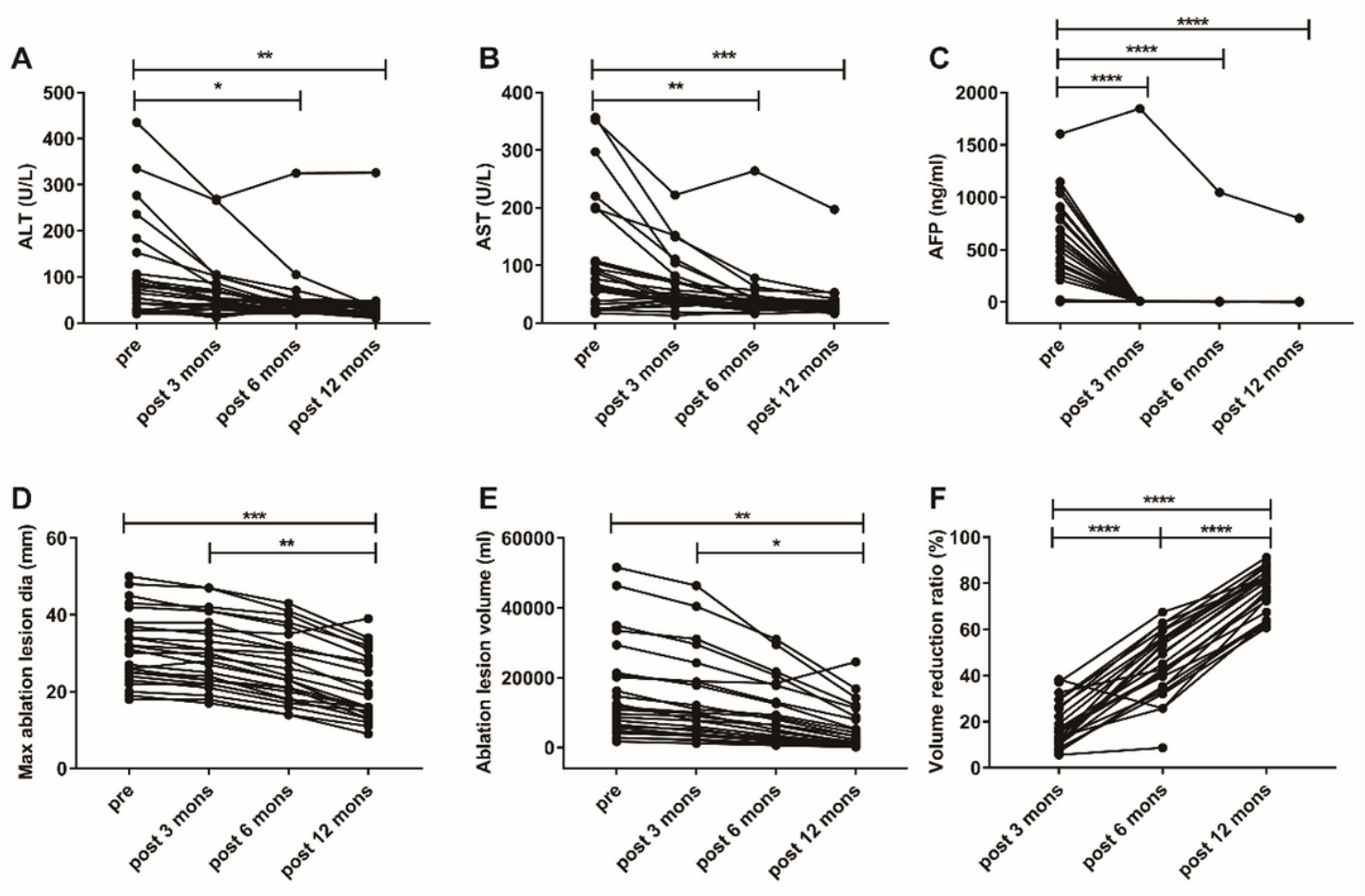


Figure 4

Clinical follow-up outcomes of precise microwave ablation. Compared with the preoperative levels, serum levels of ALT (A) and AST (B) were significantly decreased at 3 months, 6 months and 12 months postoperatively. (C) The serum level of AFP was remarkably decreased to the normal level at 3 months, 6 months and 12 months postoperatively. (D) Compared with the preoperative measurement, the maximum diameter of the ablation lesion became significantly decreased at 12 months postoperatively ($p<0.001$). (E) The volume of the ablation lesion became remarkably reduced at 12 months postoperatively ($p<0.01$). (F) The reduced ratio of the tumor volume was consistently increased at 6 months and 12 months compared to the ratio at 3 months (both $p<0.0001$)

Supplementary Files

This is a list of supplementary files associated with this preprint. Click to download.

- Supplementarydatafile1.xlsx